Title

Noncanonical HIPPO/MST Signaling via BUB3 and FOXO Drives Pulmonary Vascular Cell Growth and Survival

Journal

Circulation Research, 130(5)

ISSN

0009-7330

Authors

Kudryashova, Tatiana V
Dabral, Swati
Nayakanti, Sreenath
et al.

Publication Date

2022-03-04

DOI

10.1161/circresaha.121.319100

Peer reviewed

HHS Public Access

Author manuscript

Circ Res. Author manuscript; available in PMC 2023 March 04.

Published in final edited form as:

Circ Res. 2022 March 04; 130(5): 760–778. doi:10.1161/CIRCRESAHA.121.319100.

Non-Canonical HIPPO/MST Signaling via BUB3 and FOXO Drives Pulmonary Vascular Cell Growth and Survival

Tatiana V. Kudryashova, PhD[1,2,3,ξ], **Swati Dabral, PhD**[4,ξ], **Sreenath Nayakanti, M.Sc**[4], **Arnab Ray, BS**[2], **Dmitry A. Goncharov, BS**[1,2], **Theodore Avolio, BS**[2], **Yuanjun Shen, PhD**[1,2], **Analise Rode, BS**[2], **Andressa Pena, BS**[2], **Lifeng Jiang, PhD**[1], **Derek Lin, BS**[1], **Jeffrey Baust, BS**[2], **Timothy N. Bachman, MS**[2], **Johannes Graumann, PhD**[5], **Clemens Ruppert, PhD**[6], **Andreas Guenther, MD, PhD**[6], **Mario Schmoranzer**[4], **Yann Grobs, MSC**[7], **Sarah Eve Lemay, BSC**[7], **Eve Tremblay, BSC**[7], **Sandra Breuils-Bonnet, MSC**[7], **Olivier Boucherat, PhD**[7], **Ana L. Mora, MD**[2,3], **Horace DeLisser, MD**[8], **Jing Zhao, MD, PhD**[9], **Yutong Zhao, MD, PhD**[9], **Sébastien Bonnet, PhD**[7], **Werner Seeger, MD**[4,10], **Soni S. Pullamsetti, PhD**[4,10,*,&], **Elena A. Goncharova, PhD**[1,2,3,*,&]

[1]Lung Center, Division of Pulmonary, Critical Care and Sleep Medicine, University of California, Davis School of Medicine, Davis, CA, USA;

[2]Pittsburgh Heart, Lung and Blood Vascular Medicine Institute, University of Pittsburgh, Pittsburgh, PA, USA;

[3]Division of Pulmonary, Allergy and Critical Care Medicine, Department of Medicine, University of Pittsburgh, Pittsburgh, PA, USA;

[4]Max Planck Institute for Heart and Lung Research, Department of Lung Development and Remodeling, Member of the German Center for Lung Research (DZL), Bad Nauheim, Germany;

[5]Biomolecular Mass Spectrometry, Max Planck Institute for Heart and Lung Research, Bad Nauheim, Germany;

[6]Department of Internal Medicine, Member of the DZL, Member of CPI, Justus Liebig University, Giessen, 35392, Germany;

[7]Department of Medicine, Faculty of Medicine, Université Laval, Quebec City, Canada,

[8]Department of Pathology and Laboratory Medicine, Pulmonary Vascular Disease Program, University of Pennsylvania Perelman School of Medicine, Philadelphia, PA, USA;

[9]The Ohio State University College of Medicine, Columbus, OH, USA;

[*]**Correspondence to:** Elena Goncharova, GBSF Rm 6523, 451 Health Sciences Drive, Davis, CA 95616 Tel: 530-752-9405, eagoncharova@ucdavis.edu (or) Soni Savai Pullamsetti, Max Planck Institute for Heart and Lung Research, Park strasse 1, Bad Nauheim, Germany. Tel: +49-6032-705 380, fax: +49-6032-705 471, soni.pullamsetti@mpi-bn.mpg.de.

Author Contributions: Conception and design: EAG, SSP. Experimental work, analysis, and interpretation: TVK, SD, SN, AR, DAG, TA, YS, AR, AP, LJ, DL, JB, TNB, JG, CR, AG, MS, YG, SEL, ET, SBB, OB, ALM, HD, JZ, YZ, SB, WS, SSP, EG. Drafting the manuscript and intellectual content: EAG, SSP, TVK, SD.

[ξ]equally contributed as first authors

[&]equally contributed as senior authors

Competing Interests: None

Supplemental Materials: Expanded methods, Online Supplemental Table S1, Online Supplemental Figures S1–S17.

[10]Department of Internal Medicine, Universities of Giessen and Marburg Lung Center (UGMLC), Institute for Lung Health (ILH), Cardio-Pulmonary Institute (CPI), Member of the DZL, Justus Liebig University, Giessen, Germany

Abstract

Rationale: The mammalian Ste20-like kinases (MST) 1/2 are members of the HIPPO pathway that act as growth suppressors in adult proliferative diseases. Pulmonary arterial hypertension (PAH) manifests by increased proliferation and survival of pulmonary vascular cells in small PAs, pulmonary vascular remodeling and the rise of PA pressure. The role of MST1/2 in PAH is currently unknown.

Objective: To investigate the roles and mechanisms of the action of MST1 and MST2 in PAH.

Methods and Results: Using early-passage pulmonary vascular cells from PAH and non-diseased lungs and mice with smooth muscle (SM)-specific tamoxifen-inducible Mst1/2 knockdown, we found that, in contrast to canonical anti-proliferative/pro-apoptotic roles, MST1/2 act as pro-proliferative/pro-survival molecules in human PAH PA vascular smooth muscle cells (PAVSMC) and adventitial fibroblasts (PAAF) and support established pulmonary vascular remodeling and pulmonary hypertension (PH) in mice with SU5416/hypoxia-induced PH. By using unbiased proteomic analysis, gain- and loss-of function approaches, and pharmacological inhibition of MST1/2 kinase activity by XMU-MP-1, we next evaluated mechanisms of regulation and function of MST1/2 in PAH pulmonary vascular cells. We found that, in PAH PAAF, the pro-proliferative function of MST1/2 is caused by IL-6-dependent MST1/2 over-expression, which induces PSMC6-dependent down-regulation of FOXO3 and hyper-proliferation. In PAH PAVSMC, MST1/2 acted via forming a disease-specific interaction with BUB3 and supported extracellular matrix- and USP10-dependent BUB3 accumulation, up-regulation of Akt-mTORC1, cell proliferation, and survival. Supporting our *in vitro* observations, smooth muscle-specific Mst1/2 knockdown halted up-regulation of Akt-mTORC1 in small muscular PAs of mice with SU5416/hypoxia-induced PH.

Conclusions: Together, this study describes a novel pro-proliferative/pro-survival role of MST1/2 in PAH pulmonary vasculature, provides a novel mechanistic link from MST1/2 via BUB3 and FOXO to the abnormal proliferation and survival of PAVSMC and PAAF, remodeling and PH, and suggests new target pathways for therapeutic intervention.

Subject Terms:

Cell Signaling/Signal Transduction; Remodeling; Pulmonary Hypertension; Basic Science Research; Smooth Muscle Proliferation; Differentiation

Introduction

The mammalian Ste20-like kinases (MST) 1 and 2 (STK4/3) form the catalytic core of HIPPO, an evolutionally conserved growth-suppressor cassette[1,2]. In adult somatic cells, MST1 and 2 act as growth suppressors and protect against cancer, fibrosis, and the proliferation-driven remodeling of systemic vasculature[3–5]. MST1/2 are activated by cleavage and auto-phosphorylation at T180/183 and inhibit cell proliferation and

induce apoptosis via a broad range of mechanisms, the majority of which include phosphorylation of the large tumor suppressors (LATS)1/2 and concomitant inhibition of the transcriptional co-activators Yes-associated protein (YAP)/TAZ (WWTR1)[6], nuclear retention and activation of forkhead homeobox type O (FOXO) transcription factors[7–9], and inhibition of Akt-mTOR[2,10,11].

Pulmonary vascular remodeling due to the excessive growth of resident pulmonary vascular cells is an important component of pulmonary arterial hypertension (PAH), a progressive disease with a high mortality rate and poor prognosis[12–14], characterized by increased PA pressure, elevated right ventricular afterload, and death by heart failure[14–17]. Increased proliferation and impaired apoptosis of pulmonary arterial vascular smooth muscle cells (PAVSMC) and adventitial fibroblasts (PAAF) in small PAs from PAH lungs are supported by the constitutive activation of pro-proliferative/anti-apoptotic YAP/TAZ, Akt-mTOR axis (PAVSMC and PAAF), and the deficiency of anti-proliferative/pro-apoptotic FOXO1 (PAVSMC)[14,18–24], for which MST1 and 2 act as positive upstream regulators. Intriguingly, we previously found that MST1 and 2 have little effect on YAP/TAZ in human PAVSMC[18], and the role of MST1/2 in PAH is currently unknown.

To evaluate the roles of MST1 and 2 in PAH, we utilized tissue specimens and early-passage distal PAVSMC and PAAF from human non-diseased and PAH lungs. Human pulmonary vascular cells retain the diseased phenotype in culture, constituting a unique disease-related model for *in vitro* mechanistic studies[14,18,22,25,26]. For *in vivo* studies, we used mice carrying an inducible smooth muscle-specific Mst1/2 knockout and a SU5416/hypoxia (SuHx) model of PH, which shares several key features with human PAH including pulmonary vascular remodeling and increased PA pressure[18,27].

Methods (expanded in the Online Data Supplement).

Data Availability.

Data available on request from the authors: the data that support the findings of this study are available from the corresponding author upon reasonable request.

Human materials.

The human lung tissues (supplemental table S1) were provided by the University of Pittsburgh Medical Center Lung Transplant, Pulmonary Division Tissue Donation and the Department of Pathology Autopsy Programs in accordance with Institutional Review Board (IRB) and Clinical Training Involving Decedents (CORID) policies and by the ethics committee (Ethik Kommission am Fachbereich Humanmedizin der Justus Liebig Universität Giessen) of the University Hospital Giessen (Giessen, Germany) in accordance with national law and with the Good Clinical Practice/International Conference on Harmonisation guidelines. Primary distal PAVSMC and adventitial fibroblasts from non-diseased subjects and patients with PAH were provided by the Pulmonary Hypertension Breakthrough Initiative (PHBI), the University of Pittsburgh Vascular Medicine Institute Cell Processing Core, and by the Biobank platform of the German Center for Lung Research (DZL) under approved protocols. Cells isolation, characterization and maintenance were performed

under PHBI protocols as described in[14,18]. All experiments were repeated on primary (3–7 passage) cells from a minimum of 3 subjects. Before experiments, cells were incubated for 24–48 hours in basal media with 0.1% BSA if not stated otherwise.

Immunohistochemical, immunocytochemical, immunoblot analyses, transfection, proliferation, apoptosis, and cell count assays were performed as described in[14,18,28,29].

Animals.

All animal procedures were performed under the protocols approved by the University of Pittsburgh Animal Care and Use Committee. The following transgenic founder lines were used in this study: *Mst1fl Mst2 fl* mice (*Mst1/2*$^{fl/fl,}$ Jackson strain: *Stk4*$^{tm1.1Rjo}$ *Stk3*$^{tm1.1Rjo}$/J), SM-MHC-CreER^{T2} mice (Jackson strain: *Tg(Myh11-cre/ERT2)1Soff/J*) and the mTmG reporter mice (Jackson strain: B6,129 (Cg)-Gt(ROSA)26Sor$^{tm4(ACTB-tdTomato,-EGFP)Luo}$/J). First, male SM-MHC-CreER^{T2} mice, which express a tamoxifen-regulated Cre recombinase directed to smooth muscle cells by the *Myh 11* (SM-MHC) promoter were crossed with female mTmG reporter mice with Cre-mediated enhanced green fluorescent protein (EGFP) expression to produce male SM-MHC-CreER^{T2}/R26RmTmG offspring. Then, male SM-MHC-CreERT/R26RmTmG mice were crossed with female *Mst1/2*$^{fl/fl}$ mice to produce SM-MHC-CreER^{T2}-GFP-Mst1/2$^{f/f}$ mice (supplemental Fig. S1a,b). Treatment of SM-MHC-CreER^{T2}-GFP-Mst1/2$^{f/f}$ mice with tamoxifen results in Cre-dependent removal of floxed exons 4–5 of the *Mst1* (*Stk4*) gene and exons 5–6 of the *Mst 2* (*Stk3)* gene in smooth muscle cells and induces EGFP expression[30,31] (supplemental Fig. S1c). Because the *SM-MHC-CreER*^{T2} cassette is located in the Y chromosome, only male mice (genotype carriers) were used in further experiments. 6 to 8-week-old mice were randomly assigned to three groups. Two groups were exposed to hypoxia (10% O_2) and SU5416 (20 mg/kg, sc), (Tocris Bioscience, Bristol, UK). Injections were performed at days 0, 7 and 14 (see Fig. 5a for the experiment scheme)[14,28]. At day 17 of the experiment, mice still under hypoxia, were given injections of tamoxifen (20 mg/kg, ip, Sigma, St.Louis, MO) (SuHx-Tx group) or vehicle (SuHx-Veh group) for 5 consecutive days. After two more weeks of hypoxia exposure, blinded analysis of hemodynamic measurements was performed; animals were sacrificed, and lung tissues were collected for analysis. Negative controls included normoxia-maintained age-matched animals (CTRL group). Hemodynamic and histochemical analyses were performed as described in[14,18,32]. Blinded analysis of small PAs (25–150 μm outer diameter) was performed as described in[14,27].

Data analysis.

Immunoblots, DNA synthesis and apoptosis assays were analyzed using ImageJ (NIH, Bethesda, MD), StatView (SAS Institute, Cary, NC), STATA (StatCorp, College Station, TX) and GraphPad Prism 9.2 (GraphPad Software, San Diego, CA) software. Immunohistochemical and immunocytochemical analyses were performed using a Keyence BZ-X800 system and software (Keyence Corporation of America, Itasca, IL). Hemodynamic and morphometric data were performed using Indus Instruments (Webster, TX), IOX2 and Emka (Emka Technologies, Falls Church,VA) and Matlab (MathWorks, Natick, MA). Statistical comparisons between the two groups were performed by non-parametric Mann Whitney U test. Statistical comparisons among three or more groups were performed using

Kruskal–Wallis tests with post-hoc Dunn's pairwise comparison (all data with sample size n<6/group and skewed data with sample size n≥6/group) and one-way Analysis Of Variants (ANOVA) with Dunnett's post-hoc test for normally distributed data with sample size n≥6/group. Shapiro-Wilk normality test was used.

Results

MST1 and MST2 support increased proliferation and survival of PAVSMC and PAAF in PAH.

MST1 and MST2 act as growth suppressors in adult somatic cells by inhibiting proliferation and inducing cell differentiation or apoptosis. In order to evaluate the role of MST1 and MST2 in PAH, we first assessed functional roles of MST1 and MST2 in human PAH and non-diseased (control) pulmonary vascular cells using specific siRNAs. In agreement with published studies[14,18], PAH PAVSMC had significantly higher growth and proliferation rates compared to PAVSMC from non-diseased (control) subjects (Supplemental Figure S2). In control PAVSMC, siMST1 and siMST2 induced significant proliferation without affecting apoptosis (Fig. 1a–c). In contrast, both siMST1 and siMST2 significantly reduced proliferation and promoted significant apoptosis in PAH PAVSMC (Fig. 1a–c). Further, siMST1 and siMST2 significantly reduced proliferation of PAH PAAF, but not control PAAF and induced significant apoptosis in PAH PAAF, but not control cells (Fig. 1d–f), suggesting a pro-proliferative/pro-survival role for MST1/2 in PAH pulmonary vascular cells.

We observed no significant effects of siMST1 on the MST2 protein levels and no significant effects of siMST2 on the MST1 protein levels in PAH and control PAVSMC and PAAF (Supplemental Fig. S3). To further evaluate the potential inter-dependance of MST1 and MST2 in supporting increased growth of PAH vascular cells, we co-transfected human PAH PAVSMC and PAAF with siMST1 and siMST2. The combined depletion of MST1 and MST2 reduced PAH PAVSMC growth and proliferation compared to cells transfected with control siRNA, but did not exhibit significant additive effects in comparison to separate knockdowns (Supplemental Fig. S4 a–c). Similarly, combined transfection with siMST1 and si MST2 did not enhance the inhibitory effects of single siMST1 or siMST2 transfection on PAH PAAF proliferation (Supplemental Fig. S4d).

To support our siRNA-based findings, we next inhibited MST1/2 activity using XMU-MP-1, a selective ATP-competitive MST1/2 inhibitor[33,34]. XMU-MP-1 reduced proliferation and induced apoptosis in PAH PAVSMC and PAAF, while having little effect on control cells (Fig. 1g, h). Intriguingly, in contrast to siMST1 and siMST2 (Fig. 1a–c), XMU-MP1 did not promote proliferation of control PAVSMC (Fig. 1g), suggesting that both kinase activity and preserved protein levels may be required for MST1/2 function. Indeed, XMU-MP1 had little effect on MST1 and MST2 protein levels in control PAVSMC, while reducing MST2 protein levels in PAH PAVSMC (Supplemental Fig. S5), suggesting that the lack of XMU-MP1 effect in control cells may be, at least in part, explained by preserved MST1/2 protein levels. Interestingly, XMU-MP-1 inhibited the proliferation of PAH PA endothelial cells but did not induce apoptosis (data not shown), indicating that anti-apoptotic functions of MST1/2 in PAH may be limited to PAVSMC and PAAF cell types. In line with the inhibitor-based findings, transfection of human PAH PAVSMC with kinase-dead K59R MST1 and K56R

MST2, but not wild-type (wt) constructs (HA-MST1 and HA-MST2, denoted as wt-MST1 and wt-MST2, respectively), suppressed PAH PAVSMC proliferation compared to empty vector-transfected cells (Fig. 1i–l), reinforcing our conclusion that active MST1/2 support the proliferation and survival of PAH pulmonary vascular cells.

To determine the mechanism(s) driving the MST1/2 switch to pro-proliferative molecules in PAH pulmonary vascular cells, we next evaluated expression patterns of MST1 and MST2 in PAH patient lungs by performing a comparative analysis of human lung tissue specimens. Using immunohistochemistry and western blot analyses, we found that MST1 and MST2 are present and over-expressed in isolated PAs from PAH lungs compared to controls; increased accumulation was detected predominantly in the adventitial area (Fig. 2a, b, Supplemental Figures S6a, S7). Supporting our observations, while *MST1* and *MST2* mRNA levels were higher in both PAVSMC and PAAF from PAH lungs, only isolated PAH PAAF (but not PAH PAVSMC) had a significantly higher accumulation of MST1 and MST2 proteins compared to non-diseased cells (Fig. 2c–e, Supplemental Fig. S6b), demonstrating that MST1 and MST2 are over-accumulated in PAAF in PAH. To test the functional significance of MST1/2 over-accumulation, we transfected control PAAF with mammalian vectors expressing wt or kinase dead MST1 and MST2 and measured proliferation and apoptosis. Importantly, over-expression of wt-MST1 and wt-MST2, but not its kinase-dead mutants, significantly increased proliferation and reduced apoptosis of control PAAF compared to empty vector-transfected cells (Fig. 2f, g), suggesting that MST1/2 over-expression may be responsible for inducing PAAF proliferation and survival.

To investigate the mechanism(s) leading to increased MST1/2 expression in PAH PAAF, we next carried out *in silico* analysis of human MST1 and MST2 promoters to identify putative binding sites for PAH relevant transcription factors. Promoters of both genes showed the presence of putative binding sites for the STAT3 (Fig. 3a), a well-documented transcription factor acting downstream of several cytokine/chemokine-related[35–37] and growth factor signaling pathways,[38–40] many of which play an important role in PH pathogenesis.[41,42] To dissect the potential upstream regulator of MST1/2, we treated human non-diseased PAAF with various PH-associated cytokines (IL-6, IL-8, IL-13, IL-18, CCL2, TNF-α) and growth factors (PDGF-BB, TGF-β) and evaluated MST1/2 mRNA expression by RT PCR analysis. We found that only IL-6 stimulation led to a significant increase in both MST1 and MST2 mRNA levels compared to controls, IL-8, IL-13, IL-18, CCL2, PDGF-BB, and TGF-β had no effect or affected only MST1 or MST2, and TNF-α reduced *MST1* and *MST2* mRNA levels compared to vehicle-treated cells (Fig. 3b, Supplemental Fig. S8).

In line with the *in silico* and RT PCR analyses, stimulation with 20 ng/ml IL-6 significantly increased MST1 and MST2 protein levels in control PAAF (Fig. 3c). Further, STAT3 inhibition using a small molecule inhibitor led to a strong decrease in expression of MST1/2 in PAH PAAF while STAT1 inhibition had no significant effect (Fig. 3d, e). Collectively, our data indicate that IL-6 driven Stat3 signaling might be involved in MST1/2 upregulation in PAH PAAF. Interestingly, IL-6 had no effect on MST1 and MST2 expression in PAVSMC (Supplemental Figure S8c), suggesting that this mechanism is specific for PAAF.

Taken together, these data demonstrate that, in contrast to canonical growth-suppressor function in non-diseased pulmonary vasculature, MST1 and MST2 play a pro-proliferative, anti-apoptotic role in mesenchymal pulmonary vascular cells from PAH lungs, and that functional switch may, at least in part, be induced by IL-6/STAT3-governed overexpression.

MST1 and MST2 regulate the Akt-mTOR and FOXO axes in pulmonary vascular cells in PAH.

Canonically, MST1/2 act via inhibition of YAP/TAZ, whereas non-canonical MST1/2 act via suppression of Akt and mTORC1, or nuclear retention of FOXOs in a YAP/TAZ independent manner[1–5,8,9,11,43–45]. In agreement with published studies[14,18,19,22,26], we observed that increased proliferation of PAVSMC from patients with PAH in culture is associated with constitutive hyper-phosphorylation of Akt and ribosomal protein S6 (the molecular signature of mTORC1 activation)[14,46], and reduced FOXO1 protein content compared to non-diseased controls (supplemental Fig. S2c, d).

MST1 and 2 in human control PAVSMC appeared to signal YAP/TAZ-independently[18] and had unaltered phosphorylation of MST1/2 at T183/180 compared to controls (Supplemental Fig. S6b). Supporting our previous observations, transfection of control cells with siMST1 and siMST2 reduced the levels of pro-apoptotic protein Bim and increased S473-Akt and S6 phosphorylation rates without a marked effect on FOXO1 protein levels (Fig. 4a, b), which is in line with the previously reported growth suppressor action of MST1/2 via inhibition of Akt-mTOR[10,18]. In contrast, siRNA-induced MST1 or MST2 depletion in PAH PAVSMC resulted in accumulation of pro-apoptotic Bim and FOXO1, and reduced phosphorylation rates of Akt and S6 (Fig. 4a, b). In agreement with the siRNA-based findings, transfection with kinase-dead K59R MST1 and K56R MST2 suppressed Akt and S6 phosphorylation in PAH PAVSMC (supplemental Fig. S9). Further supporting our observations, treatment of PAH PAVSMC with MST1/2 kinase inhibitor XMU-MP-1 significantly decreased Akt and S6 phosphorylation rates and increased Bim protein content (Supplemental Fig. S10).

Interestingly, MST1 and MST2 knockdown in PAH PAAF led to an increase in protein expression of Bim and FOXO3 with no significant changes in phosphorylation of S6 and Akt (Fig. 4c, d), suggesting potentially different mechanisms of MST1/2 action in PAVSMC and PAAF from PAH lungs.

Taken together, these data show that MST1 and 2 act as pro-proliferative/pro-survival proteins in human PAH pulmonary vascular cells and promote pro-proliferative/pro-survival Akt and mTORC1 (PAVSMC) while suppressing Bim and FOXO (PAVSMC and PAAF).

Smooth muscle Mst1/2 support pulmonary vascular remodeling and PH in mice.

As increased proliferation and survival of pulmonary vascular cells play an important role in PAH pathogenesis, we next tested whether MST1/2 support PA remodeling and PH *in vivo*. To this end, we developed mice carrying a smooth muscle (SM)-specific tamoxifen-inducible *Mst1/2* knockdown cassette, which simultaneously induces cre-mediated *Mst1/2* knockdown and GFP expression in smooth muscle cells upon tamoxifen treatment (SM-MHC-CreER^{T2}GFP-Mst1/2$^{fl/fl}$) (Supplemental Fig. S1), and induced PH by combined exposure to SU5416 and hypoxia[18,27]. At days 17–21 of the experiment, mice received five

sequential injections of tamoxifen to deplete Mst1/2 (SuHx Tx group) or vehicle (SuHx Veh group) and were maintained under hypoxia for two more weeks. Controls were same-gender littermates maintained under normoxia (Fig. 5a). As expected, animals of the SuHx Veh group developed pulmonary vascular remodeling and PH as evidenced by a significant increase in PA medial thickness (PA MT) and elevated right ventricular systolic pressure (sRVP) and contractility (max dP/dT), but not systolic left ventricular pressure (sLVP) compared to controls (Fig. 5b–f, Supplemental Fig. S11). This was associated with increased phosphorylation of Akt and S6 in smooth muscle α-actin (SMA)-positive cells in small (25–150 μm) PAs (Fig. 5g, h). In contrast to vehicle-treated SuHx mice and controls, tamoxifen-treated SuHx mice showed GFP expression in SMA-positive areas of small PAs (supplemental Fig. S1c), confirming successful tamoxifen delivery to the pulmonary vasculature. In agreement with our *in vitro* findings, tamoxifen-induced SM-specific Mst1/2 depletion (SuHx Tx group) reversed pulmonary vascular remodeling (PA MT) (Fig. 5b, c), decreased Akt and S6 phosphorylation (Fig. 5g, h), and attenuated overall PH (sRVP and max dP/dT) when compared to the vehicle-treated (SuHx Veh) group without affecting sLVP (Fig. 5d–f, supplemental Fig. S11). These data show that smooth muscle Mst1/2 support pulmonary vascular remodeling and experimental PH *in vivo*.

MST1/2 in PAH PAVSMC form disease-specific interaction with the cell cycle protein BUB3.

Because PAVSMC from PAH lungs did not demonstrate MST1 or 2 accumulation or changes in T180/183 phosphorylation status (Supplemental Fig. S6), we hypothesized that the observed switch in MST1/2 function is caused by PAH-specific protein-protein interactions. To test this hypothesis, we immuno-precipitated MST1 and MST2 from control and PAH PAVSMC and performed mass spectrometry analysis (Fig. 6a). It revealed that MST1 and MST2 form different interactomes in PAH and non-diseased PAVSMC, and identified 13 proteins that interact with MST1 exclusively in PAH, but not control PAVSMC (Fig. 6b left panel). Out of these 13 proteins, only BUB3 and 60S ribosomal protein L22-like 1 (RPL22L1) also interacted with MST2 exclusively in PAH cells (Fig. 6b right panel). To test functional selectivity of BUB3 and RPL22L1 toward PAH, we depleted those proteins with specific siRNAs and performed a cell growth assay. We found that the depletion of BUB3 reduced growth of PAH, but not control PAVSMC, while the depletion of RPL22L1 decreased growth of both, control and PAH cells (Fig. 6c), showing that only BUB3 acts in a PAH-specific manner. Interestingly, we did not observe any significant interaction between BUB3 and MST1/2 in co-IP studies in PAH PAAF (data not shown), suggesting cell-type-specific mechanisms for MST1/2 action.

MST1/2 promote BUB3 accumulation in PAH PAVSMC via ECM and USP10.

BUB3 is a cell cycle protein that promotes mitotic entry[47] and acts as a member of the mitotic checkpoint complex (MCC), a component of the spindle assembly checkpoint (SAC)[48]. The mechanism(s) promoting BUB3 accumulation in PAH is unknown. Since MST1 is involved in both, regulating accurate kinetochore-microtubule attachment[49] and mechanosensing, we hypothesized that MST1/2 support pro-proliferative signaling by promoting BUB3 accumulation via modulating the extracellular matrix (ECM). To test this hypothesis, we first treated human PAH PAVSMC with MST1/2 inhibitor XMU-MP-1 and observed a significant ~2-fold decrease in BUB3 protein levels (Fig. 6d). Next, we

plated control PAVSMC on the decellularized matrices produced by non-diseased (control) or PAH PAVSMC (Fig. 6e) and found that control cells, grown on PAH PAVSMC-produced matrices, had significantly higher BUB3 protein levels (Fig. 6g). This was accompanied by elevated cell growth compared to cells grown on the matrices produced by control PAVSMC (Fig. 6f). PAH PAVSMC treated with XMU-MP-1 produced reduced amounts of two major PAH-specific ECM proteins, fibronectin (FN) and collagen 1 (Col1A) (data not shown), indicating the importance of MST1/2 in ECM production. Importantly, control PAVSMC, plated on the matrices produced by XMU-MP-1-treated PAH PAVSMC, showed reduced cell growth (Fig. 6h, i) and decreased protein levels of BUB3 (Fig. 6j) compared to the cells grown on the matrices produced by vehicle-treated PAH PAVSMC. Further supporting the relevance of our findings to human PAH, we found that BUB3 protein levels are significantly higher in SMA-positive areas of small remodeled PAs in human PAH lungs and isolated early-passage human PAH PAVSMC as compared to non-diseased controls (Fig. 7a, b). Together, these data demonstrate that MST1/2 control the accumulation of BUB3 in PAH PAVSMC by modifying ECM.

In addition to the ECM, proliferation of PAVSMC in PAH could be induced by various soluble pro-PAH mitogens, including pro-inflammatory cytokines and growth factors[18,22,35]. To test whether soluble pro-PAH factors could also induce PAH-specific MST1/2-dependent signaling in human PAVSMC, we treated non-diseased (control) PAVSMC with IL-6, IL-8, IL-13, IL-18, CCL2, TNF-α, PDGF-BB, or TGF-β and examined BUB3 protein levels and Akt phosphorylation status using immunoblot analysis. In agreement with published studies[50–52], IL-13, PDGF, TGF-β, and TNF-α increased pAkt/Akt ratio in control PAVSMC. However, none of the analyzed agonists induced accumulation of BUB3 similar to what was seen in PAH PAVSMC (Supplemental Figure S12), suggesting that MST1/2-induced BUB3 accumulation in PAH PAVSMC is likely growth factors- and cytokine-independent.

Beyond BUB3, our screen of the MST1/2 PAH-specific interactome (Fig. 6b) produced the deubiquitinating enzyme (DUB) ubiquitin-specific peptidase 10 (USP10) as another interactor of MST1 and MST2 enriched in PAH. Interestingly, we observed increased protein levels of USP10 in PAH PAVSMC and small PAs from PAH lungs compared to controls (Fig. 7b, Supplemental Figure S13), and siRNA mediated knockdown of USP10 in PAH PAVSMC resulted in decreased BUB3 expression that was induced by MST1 and, to a lesser extent, MST2 overexpression (Fig. 7c–h). These findings may be interpreted as BUB3 interacting with USP10 in the presence of MST1/2, which, in turn, increases the BUB3 protein level by interfering with its degradation.

BUB3 drives PAH PAVSMC proliferation, survival, and activation of Akt-mTORC1.

BUB3 knockdown is known to abrogate SAC, promote apoptosis and inhibit proliferation of tumor cells[53]. We found that siRNA-induced BUB3 depletion significantly reduced proliferation and induced apoptosis in PAH, but not control PAVSMC (Fig. 7i), showing that BUB3 is required for increased proliferation and survival of human PAH PAVSMC.

BUB3 is a member of the Akt1 interactome[54]. Akt1 is a pro-proliferative/pro-survival protein-kinase that positively regulates mTORC1[21,55–57]. Because Akt and mTORC1 are

up-regulated in PAH PAVSMC in an MST1/2-dependent manner (Fig. 4a, b, Supplemental Fig. S9, S10) and are required for PAVSMC remodeling[14,19,58–61], we reasoned that BUB3 may regulate PAH PAVSMC proliferation and survival via Akt-mTORC1. Transfection of PAH PAVSMC with siRNA BUB3 significantly decreased Akt phosphorylation and mTORC1-specific phosphorylation of S6 (Fig. 7j), suggesting that BUB3 is required for the activation of the Akt-mTOR axis in PAH PAVSMC. To test whether MST1/2 act via BUB3, we transfected PAH PAVSMC with a vector expressing human BUB3 (pCMV6-BUB3) or an empty pCMV6 plasmid, and examined cell proliferation and apoptosis in the presence or absence of the MST1/2 kinase inhibitor XMU-MP-1. We found that over-expression of BUB3 moderately attenuates XMU-MP-1-dependent inhibition of proliferation and protects from XMU-MP-1-induced apoptosis (Fig. 7k). Together, these data suggest that MST1/2 promote BUB3 over-accumulation in PAH PAVSMC in an USP10-dependent manner, leading to BUB3-dependent maintenance of increased proliferation, survival, and activation of Akt-mTORC1 in PAH PAVSMC (Fig. 7l). Interestingly, BUB3 silencing did not affect FOXO1 protein levels (data not shown), suggesting that the regulation of FOXOs by MST1/2 may be BUB3-independent.

MST1/2 promote PAAF proliferation and survival via PSMC6-dependent inhibition of FOXO3.

Based on our observation of MST1/2 knockdown-mediated upregulation of FOXO3 in PAH PAAF (Fig. 4c, d), we hypothesized that increased MST1/2 downregulate FOXO3 in PAH PAAF resulting in hyperproliferation and increased survival. In concurrence, HEK 293 cells transfected with MST1/2 wt plasmids showed an increased nuclear exclusion of FOXO3 compared to an empty vector, as well as their respective kinase dead mutants (Fig. 8a, Supplemental Fig. S14a) as measured by nuclear-cytoplasmic fractionation followed by western blotting. Further, a luciferase assay employing FOXO3 dependent luciferase reporter plasmid, containing three copies of FOXO response elements (FHRE), showed a significant decrease in luciferase activity under MST1/2 wt plasmids; the effect was attenuated under overexpression of kinase dead mutants (Fig. 8b). Conversely, knockdown of both MST1 and MST2 resulted in an increased nuclear inclusion of FOXO3 with a concomitant increase in FHRE luciferase activity (Fig. 8c, d, Supplemental Fig. S14b). To analyze how much the pro-proliferative and pro-survival effect of MST1/2 is mediated by selectively inhibiting FOXO3, we carried out a dual knockdown of MST1/2 and FOXO3. We observed that the FOXO3 knockdown reversed the decrease in proliferation seen in PAH PAAF treated with siMST1 and siMST2 (Fig. 8e). Additionally, the FOXO3 knockdown was able to substantially reverse the apoptotic effect of MST1/2 knockdown (Fig. 8f). These findings signify that the majority of anti-proliferative and pro-apoptotic effects of MST1/2 is mediated via FOXO3. In further support, we observed a decreased expression of FOXO3 in PAH PAAF compared to control cells (Supplemental Fig. S15a), and the FOXO3 knockdown itself increased proliferation and survival of control PAAF (Supplemental Fig. S15b, c).

To investigate the mechanism of FOXO3 regulation by MST1/2, we immunoprecipitated FOXO3-FLAG from MST1/2 wt and kinase dead mutants overexpressing HEK cells and performed mass spectrometric analysis for post translational modifications and

interacting partners (Supplemental Fig. S15d). We did not detect significant changes in post translational modifications; however, we obtained differential interacting partners of FOXO3 in the presence of wt MST1/2 or their kinase dead mutants. PSMC6, an essential component of the assembled 19S proteasome subunit, was revealed as the top interacting partner for FOXO3 in the presence of MST1 and among the top 10 in presence of MST2, while it did not show any interaction with FOXO3 in the presence of kinase dead mutants (Supplemental Fig. S15e). We carried out co-immunoprecipitation studies with a FOXO3 pulldown in the presence of a MST1/2 knockdown to confirm these findings. We were indeed able to observe an interaction between FOXO3 and PSMC6 which was abrogated on the MST1/2 knockdown (Fig. 8g). Further, a siRNA mediated knockdown of PSMC6 resulted in restoring FOXO3 expression reduced by MST1 overexpression (Fig. 8h, i). PSMC6 belongs to the AAA (ATPases associated with diverse cellular activities) proteins which unfold ubiquitinated target proteins for translocation into the proteolytic chamber of the proteasome leading to degradation[62]. Collectively, our findings strongly suggest that FOXO3 interacts with the proteasome complex in the presence of MST1/2, leading to its degradation, and ultimately contributing to the hyperproliferative and pro-survival phenotype of PAH PAAF (Fig. 8j).

Discussion

We here report that MST1 and MST2 act as pro-proliferative pro-survival proteins in PAH. Our novel findings (Supplemental Fig. S16) are: (i) MST1 and 2 are upregulated in human PAH PAAF; (ii) inflammatory cytokine IL-6, involved in the pathogenesis of PAH, promotes MST1 and MST2 expression in PAAF; (iii) in contrast to the well-described canonical growth-suppressor function, MST1 and 2 act as pro-proliferative/pro-survival molecules in human PAH PAVSMC and PAAF; (iv) a distinct MST1 and 2 PAH-specific interactomes direct pro-proliferative/pro-survival signaling in human PAH PAVSMC and PAAF via BUB3 and FOXO3, respectively; and (v) genetic ablation of Mst1/2 in mice suppresses pulmonary vascular remodeling and attenuates SuHx-induced PH *in vivo*.

MST1 and 2 are core kinases of the HIPPO growth-suppressor cassette. We observed that, under normal conditions, MST1 and MST2 inhibit proliferation of human microvascular PAVSMC. This is in agreement with previous reports of the growth-suppressor function of MST1/2 in the heart, lungs, and cancers[1,6,63,64]. However, in contrast to healthy PAVSMC and PAAF, MST1 and 2 act as pro-proliferative/pro-survival molecules in diseased (i.e. PAH) human pulmonary vascular cells. Both gain and loss of function studies indicated pro-proliferative and pro-survival effects of MST1 and 2 in PAH PAVSMC and PAAF. Corroborating our *in vitro* data, the smooth muscle-specific Mst1/2 double knockout in mice attenuated SuHx-induced vascular remodeling and PH, indicating pro-remodeling and pro-PH roles for Mst1/2 *in vivo*.

This non-canonical, pro-proliferative role of MST1 and 2 could be explained mechanistically by formation of context-specific MST1- and 2-dependent interactomes. Specifically, we identified that, firstly, MST1/2 forms a PAH-specific interaction with cell cycle protein BUB3 and USP10, promoting the accumulation of BUB3 and consequent up-regulation of pro-proliferative pro-survival Akt and mTORC1 in PAH PAVSMC.

Secondly, we found that MST1/2-driven PAH-specific FOXO3-PSMC6 interaction leads to proteasomal degradation of FOXO3, permitting activation of pro-proliferative and pro-survival genes in PAH PAAF. Lastly, distinct pro-PAH stimuli (i.e. ECM in PAVSMCs and IL-6 in PAAFs) led to the formation of differential protein-protein interactions (MST-BUB3-USP10 in PAH PAVSMCs and MST-FOXO3-PSMC6 in PAH PAAFs). These lines of evidence indicate that PAH-specific MST1/2 interactomes determine the predominance of pro-proliferative over the growth-suppressive responses of MST kinases in PAH pulmonary vascular cells; and that distinct PAH-specific stimuli support interaction of MST with different proteins, leading to cell type-specific pro-proliferative signaling in PAH PAVSMCs versus PAH PAAFs.

One of the interesting findings of this study is the interaction between MST and the mitotic checkpoint protein BUB3, and the MST-mediated upregulation of BUB3 exclusively in the PAH setting. Of note, a marked upregulation of BUB3 in PAH human lung tissues and *ex vivo* cultured PAVSMC was also observed. BUB3 regulates mitotic exit via quality control of microtubular attachment and chromosome segregation[65–67]. In line with our data, increased protein levels of BUB3 in several human cancers are associated with poor prognosis[68,69], suggesting a potential role of BUB3 in hyper-proliferation. Importantly, BUB3 knockdown in PAH PAVSMC potently reversed the hyper-proliferative and apoptosis-resistant phenotype by modulating Akt and mTORC1 signaling pathways, suggesting that BUB3 functions as a novel downstream mediator of MST kinases in regulating pulmonary vascular cell proliferation.

MST1/2 support increased BUB3 protein levels in PAH PAVSMC via ECM, suggesting that MST kinases cooperate with ECM proteins to increase the protein stability of BUB3 and subsequently the mitotic checkpoint signaling. In this study, we also identified USP10 as a novel deubiquitinase that can stabilize BUB3 and block its degradation in PAH. In addition, upregulation of USP10 protein content, concomitant with increased BUB3 in PAH PAVSMC, suggests that a PAH-specific MST1/2 interactome leads to an accumulation of BUB3. Collectively, our study provides new insight into the regulatory mechanism of BUB3 and mitotic checkpoint signaling in PAH and uncovers the MST1/2-USP10-BUB3 axis as a major regulator of pro-proliferative/pro-survival functions of PAH PAVSMC.

Another interesting finding of this study is a distinct mode of the regulation of FOXO transcription factors by the MST family of kinases. FOXO transcription factors are critical integrators of multiple signaling pathways in pulmonary vascular cells and serve as central downstream effectors in driving PAH and fibrogenesis[22,70]. We identified pro-PAH IL-6/STAT3 signaling as an activator of MST1 and MST2 which, in turn, promote the interaction of FOXO3 with the PSMC6 proteasome complex. The MST1- and MST2-induced interaction of PSMC6 with FOXO3 inhibited the translocation of FOXO3 to the nucleus and promoted FOXO3 degradation, thereby inducing PAAF proliferation and survival. These findings were further supported by the decreased expression of FOXO3 in PAH PAAF. To our knowledge, this is the first study that demonstrates a negative regulation of FOXO proteins by MST kinases, which is in contrast to previous research that suggested a positive regulation of FOXO proteins by MST kinases. Lehtinen et al. demonstrated that under conditions of oxidative stress MST1 is activated and, in turn, phosphorylates

FOXO3 at serine 207, disrupting FOXO3 interaction with 14-3-3 protein, promoting FOXO3 translocation to the nucleus, and thereby inducing neuronal cell death[8,71]. However, in our experiments, MST failed to phosphorylate the forkhead domain of FOXO proteins (data not shown), suggesting that MST kinases-mediated FOXO regulation is cellular- and pathophysiological context-specific. Taken together, our findings demonstrate an intimate signaling link between MST kinases and FOXO transcription factors that regulate hyper-proliferation.

Notably, we found that kinase-dead mutants as well as a pharmacological inhibitor of MST1 and 2 abrogated PAH-specific MST signaling and subsequent pro-proliferative/pro-survival effects. However, T183 and T180 autophosphorylation sites, required for canonical MST1/2 signaling (i.e. activation of LATS and inactivation of YAP/TAZ), are unaltered in PAH cells compared to controls. Apart from autophosphorylation, MST1/2 can be activated via trans-phosphorylation by protein kinases (i.e. AKT and c-Abl) and by protein-protein interactions. For example, MOB3A/B/C adaptor proteins were found to associate with MST1 and negatively regulate MST1-mediated apoptosis, supporting tumorigenesis in glioblastoma multiform and pancreatic cancer[60,72]. Furthermore, interaction with BUB3 (as identified in this study) as well as interaction with mTORC[14] and SARAH domain binding proteins such as RASSF1[73] may regulate the MST kinase activity.

In summary, the present study provides strong evidence that MST1/2 kinases are activated in the medial and adventitial layers of small PAs, form PH-specific protein-protein interactions with BUB3 and FOXO, and function as pro-proliferative and pro-survival proteins centrally involved in the pathogenesis of PAH. Thus, inhibition of MST1 and 2 kinase activity provides a potential new therapeutic option to reverse the vascular remodeling and overall PH.

Supplementary Material

Refer to Web version on PubMed Central for supplementary material.

Acknowledgments

We thank the Biostatistics, Epidemiology, and Research Design program at the Clinical and Translational Science Center, University of California, Davis for their help with statistical analysis.

Sources of funding:

This work is supported by NIH/NHLBI R01HL113178 (EAG), R01HL130261 (EAG), R01HL150638 (EAG), 5P01HL103455-05 (ALM, EAG), SFB-1213 (Projekt nummer 268555672) projects A01 and A05 (SSP), Excellence Cluster ECCPS/CPI (SSP), R01HL151513-01 (JZ). The Pulmonary Hypertension Breakthrough Initiative is supported by NIH/NHLBI R24HL123767.

Non-standard Abbreviations and Acronyms

BrdU	Bromodeoxyuridine
EGFP	Enhanced Green Fluorescent Protein
ECM	Extracellular Matrix

FOXO	Forkhead Homeobox Type O
FHRE	Foxo Response Elements
IPAH	Idiopathic PAH
MST	Mammalian Ste20-Like Kinase
MCC	Mitotic Checkpoint Complex
MHC	Myosin Heavy Chain
PAAF	Pulmonary Arterial Adventitial Fibroblast
PAH	Pulmonary Arterial Hypertension
PAP	Pulmonary Arterial Pressure
PAVSMC	Pulmonary Arterial Vascular Smooth Muscle Cells
PA	Pulmonary Artery
PA MT	Pulmonary Artery Medial Thickness
PAH	Pulmonary Arterial Hypertension
PH	Pulmonary Hypertension
STK	Serine/Threonine Kinase
SM	Smooth Muscle
SMA	Smooth Muscle alpha-Actin
SAC	Spindle Assembly Checkpoint
SuHx	SU5416/Hypoxia
sLVP	Systolic Left Ventricular Pressure
sRVP	Systolic Right Ventricular Pressure
TUNEL	Terminal Deoxynucleotidyl Transferase dUTP Nick End Labeling
wt	Wild Type

References

1. Johnson R & Halder G. The two faces of Hippo: targeting the Hippo pathway for regenerative medicine and cancer treatment. Nat Rev Drug Discov. 2014;13:63–79. [PubMed: 24336504]
2. Cinar B, Fang P-K, Lutchman M, Di Vizio D, Adam RM, Pavlova N, Rubin MA, Yelick PC & Freeman MR. The pro-apoptotic kinase Mst1 and its caspase cleavage products are direct inhibitors of Akt1. EMBO J. 2007;26:4523–4534. [PubMed: 17932490]
3. Pan D The Hippo Signaling Pathway in Development and Cancer. Devl Cell. 2010;19:491–505.

4. Ono H, Ichiki T, Ohtsubo H, Fukuyama K, Imayama I, Hashiguchi Y, Sadoshima J & Sunagawa K. Critical Role of Mst1 in Vascular Remodeling After Injury. Arterioscler Thromb Vasc Biol. 2005;25:1871–1876. [PubMed: 15961701]
5. Del Re DP, Matsuda T, Zhai P, Gao S, Clark GJ, Van Der Weyden L & Sadoshima J. Proapoptotic Rassf1A/Mst1 signaling in cardiac fibroblasts is protective against pressure overload in mice. J Clin Invest. 2010;120:3555–3567. [PubMed: 20890045]
6. Gomez M, Gomez V & Hergovich A. The Hippo pathway in disease and therapy: cancer and beyond. Clin Transl Med. 2014;3:22. [PubMed: 25097725]
7. Jang S-W, Yang S-J, Srinivasan S & Ye K. Akt Phosphorylates MstI and Prevents Its Proteolytic Activation, Blocking FOXO3 Phosphorylation and Nuclear Translocation. J Biol Chem. 2007;282:30836–30844. [PubMed: 17726016]
8. Lehtinen MK, Yuan Z, Boag PR et al. A Conserved MST-FOXO Signaling Pathway Mediates Oxidative-Stress Responses and Extends Life Span. Cell. 2006;125:987–1001. [PubMed: 16751106]
9. Valis K, Prochazka L, Boura E et al. Hippo/Mst1 Stimulates Transcription of the Proapoptotic Mediator NOXA in a FoxO1-Dependent Manner. Cancer Res. 2011;71:946–954. [PubMed: 21245099]
10. Chao Y, Wang Y, Liu X et al. Mst1 regulates glioma cell proliferation via the AKT/mTOR signaling pathway. J Neurooncol. 2015;121:279–288. [PubMed: 25373346]
11. Romano D, Matallanas D, Weitsman G, Preisinger C, Ng T & Kolch W. Proapoptotic Kinase MST2 Coordinates Signaling Crosstalk between RASSF1A, Raf-1, and Akt. Cancer Res. 2010;70:1195–1203. [PubMed: 20086174]
12. Humbert M, Morrell NW, Archer SL et al. Cellular and molecular pathobiology of pulmonary arterial hypertension. J Am Coll Cardiol. 2004;43:S13–S24.
13. Erzurum SC, Rounds SI, Stevens T et al. Strategic Plan for Lung Vascular Research: An NHLBI-ORDR Workshop Report. Am J Respir Crit Care Med. 2010;182:1554–1562. [PubMed: 20833821]
14. Goncharov DA, Kudryashova TV, Ziai H, Ihida-Stansbury K, DeLisser H, Krymskaya VP, Tuder RM, Kawut SM & Goncharova EA. Mammalian target of rapamycin complex 2 (mTORC2) coordinates pulmonary artery smooth muscle cell metabolism, proliferation, and survival in pulmonary arterial hypertension. Circulation. 2014;129:864–874. [PubMed: 24270265]
15. Rabinovitch M Molecular pathogenesis of pulmonary arterial hypertension. The J Clin Invest. 2012;122:4306–4313. [PubMed: 23202738]
16. West JD, Austin ED, Gaskill C et al. Identification of a common Wnt-associated genetic signature across multiple cell types in pulmonary arterial hypertension. Am J Physiol Cell Physiol. 2014;307:415–430.
17. Morrell NW, Adnot S, Archer SL et al. Cellular and Molecular Basis of Pulmonary Arterial Hypertension. J Am Coll Cardiol. 2009;54:S20–S31. [PubMed: 19555855]
18. Kudryashova TV, Goncharov DA, Pena A et al. HIPPO–Integrin-linked Kinase Cross-Talk Controls Self-Sustaining Proliferation and Survival in Pulmonary Hypertension. Am J Respir Crit Care Med. 2016;194:866–877. [PubMed: 27119551]
19. Bertero T, Cottrill KA, Lu Y et al. Matrix Remodeling Promotes Pulmonary Hypertension through Feedback Mechanoactivation of the YAP/TAZ-miR-130/301 Circuit. Cell Rep. 2015;13:1016–1032. [PubMed: 26565914]
20. Dieffenbach PB, Haeger CM, Coronata AMF, Choi KM, Varelas X, Tschumperlin DJ & Fredenburgh LE. Arterial stiffness induces remodeling phenotypes in pulmonary artery smooth muscle cells via YAP/TAZ-mediated repression of cyclooxygenase-2. Am J Physiol Lung Cell Mol Physiol. 2017;313:L628–L647. [PubMed: 28642262]
21. Pullamsetti SS, Savai R, Seeger W & Goncharova EA. Translational Advances in the Field of Pulmonary Hypertension.From Cancer Biology to New Pulmonary Arterial Hypertension Therapeutics. Targeting Cell Growth and Proliferation Signaling Hubs. Am J Respir Crit Care Med. 2017;195:425–437. [PubMed: 27627135]

22. Savai R, Al-Tamari HM, Sedding D et al. Pro-proliferative and inflammatory signaling converge on FoxO1 transcription factor in pulmonary hypertension. Nat Med. 2014;20:1289. [PubMed: 25344740]
23. Chai X, Sun D, Han Q, Yi L, Wu Y & Liu X. Hypoxia induces pulmonary arterial fibroblast proliferation, migration, differentiation and vascular remodeling via the PI3K/Akt/p70S6K signaling pathway. Int J Mol Med. 2018;41:2461–2472. [PubMed: 29436587]
24. Stenmark KR, Gerasimovskaya E, Nemenoff RA & Das M. Hypoxic Activation of Adventitial Fibroblasts*: Role in Vascular Remodeling. Chest. 2002;122:326S–334S. [PubMed: 12475810]
25. Kudryashova TV, Goncharov DA, Pena A, Ihida-Stansbury K, DeLisser H, Kawut SM & Goncharova EA. Profiling the role of mammalian target of rapamycin in the vascular smooth muscle metabolome in pulmonary arterial hypertension. Pulm Circ. 2015;5:667–680. [PubMed: 26697174]
26. Boucherat O, Chabot S, Paulin R et al. HDAC6: A Novel Histone Deacetylase Implicated in Pulmonary Arterial Hypertension. Sci Rep. 2017;7:4546–4546. [PubMed: 28674407]
27. Vitali SH, Hansmann G, Rose C, Fernandez-Gonzalez A, Scheid A, Mitsialis SA & Kourembanas S. The Sugen 5416/hypoxia mouse model of pulmonary hypertension revisited: long-term follow-up. Pulm Circ. 2014;4:619–629. [PubMed: 25610598]
28. Krymskaya VP, Snow J, Cesarone G et al. mTOR is required for pulmonary arterial vascular smooth muscle cell proliferation under chronic hypoxia. FASEB J. 2011:25:1922–1933. [PubMed: 21368105]
29. Goncharova EA, Goncharov DA & Krymskaya VP. Assays for in vitro monitoring of human airway smooth muscle (ASM) and human pulmonary arterial vascular smooth muscle (VSM) cell migration. Nat Protocols. 2007;1:2933–2939.
30. Herring BP, Hoggatt AM, Burlak C & Offermanns S. Previously differentiated medial vascular smooth muscle cells contribute to neointima formation following vascular injury. Vasc Cell. 2014;6:21–21. [PubMed: 25309723]
31. Chen Q, Zhang H, Liu Y et al. Endothelial cells are progenitors of cardiac pericytes and vascular smooth muscle cells. Nat Commun. 2016;7:12422. [PubMed: 27516371]
32. Kelley EE, Baust J, Bonacci G et al. Fatty acid nitroalkenes ameliorate glucose intolerance and pulmonary hypertension in high-fat diet-induced obesity. Cardiovasc Res. 2014;101:352–363. [PubMed: 24385344]
33. Fan F, He Z, Kong L-L et al. Pharmacological targeting of kinases MST1 and MST2 augments tissue repair and regeneration. Sci Transl Med. 2016;8:352ra108–352ra108.
34. Qu J, Zhao H, Li Q, Pan P, Ma K, Liu X, Feng H & Chen Y. MST1 Suppression Reduces Early Brain Injury by Inhibiting the NF-κB/MMP-9 Pathway after Subarachnoid Hemorrhage in Mice. Behav Neurol. 2018;2018:6470957–6470957. [PubMed: 30018671]
35. Pullamsetti SS, Seeger W & Savai R. Classical IL-6 signaling: a promising therapeutic target for pulmonary arterial hypertension. J Clin Invest. 2018;128:1720–1723. [PubMed: 29629898]
36. Hillmer EJ, Zhang H, Li HS & Watowich SS. STAT3 signaling in immunity. Cytokine Growth Factor Rev. 2016;31:1–15. [PubMed: 27185365]
37. Garg M, Shanmugam MK, Bhardwaj V et al. The pleiotropic role of transcription factor STAT3 in oncogenesis and its targeting through natural products for cancer prevention and therapy. Med Res Rev. 2021;41:1291–1336.
38. Li L, Xu M, Li X et al. Platelet-derived growth factor-B (PDGF-B) induced by hypoxia promotes the survival of pulmonary arterial endothelial cells through the PI3K/Akt/Stat3 pathway. Cell Physiol Biochem. 2015;35:441–451. [PubMed: 25613241]
39. Pullamsetti SS, Berghausen EM, Dabral S et al. Role of Src tyrosine kinases in experimental pulmonary hypertension. Arterioscler Thromb Vasc Biol. 2012;32:1354–1365. [PubMed: 22516066]
40. Liu RY, Zeng Y, Lei Z, Wang L, Yang H, Liu Z, Zhao J & Zhang HT. JAK/STAT3 signaling is required for TGF-β-induced epithelial-mesenchymal transition in lung cancer cells. Int J Oncol. 2014;44:1643–1651. [PubMed: 24573038]

41. Soon E, Holmes AM, Treacy CM et al. Elevated levels of inflammatory cytokines predict survival in idiopathic and familial pulmonary arterial hypertension. Circulation. 2010;122:920–927. [PubMed: 20713898]
42. Groth A, Vrugt B, Brock M, Speich R, Ulrich S & Huber LC. Inflammatory cytokines in pulmonary hypertension. Respir Res. 2014;15:47. [PubMed: 24739042]
43. Collak FK, Yagiz K, Luthringer DJ, Erkaya B & Cinar B. Threonine-120 Phosphorylation Regulated by Phosphoinositide-3-Kinase/Akt and Mammalian Target of Rapamycin Pathway Signaling Limits the Antitumor Activity of Mammalian Sterile 20-Like Kinase 1. J Biol Chem. 2012;287:23698–23709. [PubMed: 22619175]
44. Lin Z, Zhou P, von Gise A et al. Pi3kcb links Hippo-YAP and PI3K-AKT signaling pathways to promote cardiomyocyte proliferation and survival. Circ Res. 2015;116:35–45. [PubMed: 25249570]
45. Ye X, Deng Y & Lai Z-C. Akt is negatively regulated by Hippo signaling for growth inhibition in Drosophila. Dev Biol. 2012;369:115–123. [PubMed: 22732571]
46. Goncharova EA. mTOR and vascular remodeling in lung diseases: current challenges and therapeutic prospects. FASEB J. 2013;27:1796–1807. [PubMed: 23355268]
47. Lopes CS, Sampaio P, Williams B, Goldberg M & Sunkel CE. The Drosophila Bub3 protein is required for the mitotic checkpoint and for normal accumulation of cyclins during G2 and early stages of mitosis. J Cell Sci. 2005;118:187–198. [PubMed: 15615783]
48. Logarinho E & Bousbaa H. Kinetochore-microtubule interactions “in check” by Bub1, Bub3 and BubR1: The dual task of attaching and signalling. Cell Cycle. 2008;7:1763–1768. [PubMed: 18594200]
49. Yang S, Zhang L, Chen X, Chen Y & Dong J. Oncoprotein YAP regulates the spindle checkpoint activation in a mitotic phosphorylation-dependent manner through up-regulation of BubR1. J Biol Chem. 2015;290:6191–6202. [PubMed: 25605730]
50. Goncharova EA, Ammit AJ, Irani C, Carroll RG, Eszterhas AJ, Panettieri RA & Krymskaya VP. PI3K is required for proliferation and migration of human pulmonary vascular smooth muscle cells. Am J Physiol Lung Cell Mol Physiol. 2002;283:L354–363. [PubMed: 12114197]
51. Suwanabol PA, Seedial SM, Zhang F, Shi X, Si Y, Liu B & Kent KC. TGF-β and Smad3 modulate PI3K/Akt signaling pathway in vascular smooth muscle cells. Am J Physiol Heart Circ Physiol. 2012;302:H2211–H2219. [PubMed: 22447946]
52. Desai LP, Wu Y, Tepper RS & Gunst SJ. Mechanical stimuli and IL-13 interact at integrin adhesion complexes to regulate expression of smooth muscle myosin heavy chain in airway smooth muscle tissue. Am J Physiol Lung Cell Mol Physiol. 2011;301:L275–L284. [PubMed: 21642449]
53. Prinz F, Puetter V, Holton SJ et al. Functional and Structural Characterization of Bub3·BubR1 Interactions Required for Spindle Assembly Checkpoint Signaling in Human Cells. J Biol Chem. 2016;291:11252–11267. [PubMed: 27030009]
54. Duggal S, Jailkhani N, Midha MK, Agrawal N, Rao KVS & Kumar A. Defining the Akt1 interactome and its role in regulating the cell cycle. Sci Rep. 2018;8:1303. [PubMed: 29358593]
55. Ou C, Sun Z, Li S, Li G, Li X & Ma J. Dual roles of yes-associated protein (YAP) in colorectal cancer. Oncotarget. 2017;8:75727–75741. [PubMed: 29088905]
56. Csibi A & Blenis J. Hippo–YAP and mTOR pathways collaborate to regulate organ size. Nat Cell Biol. 2012;14:1244. [PubMed: 23196842]
57. Hay N Interplay between FOXO, TOR, and Akt. Biochim Biophys Acta. 2011;1813:1965–1970. [PubMed: 21440577]
58. Houssaini A, Abid S, Mouraret N et al. Rapamycin Reverses Pulmonary Artery Smooth Muscle Cell Proliferation in Pulmonary Hypertension. Am J Respir Cell Mol Biol. 2013;48:568–577. [PubMed: 23470622]
59. Pena A, Kobir A, Goncharov D et al. Pharmacological Inhibition of mTOR Kinase Reverses Right Ventricle Remodeling and Improves Right Ventricle Structure and Function in Rats. Am J Respir Cell Mol Biol. 2017;57:615–625. [PubMed: 28679058]
60. Tang H, Chen J, Fraidenburg DR et al. Deficiency of Akt1, but not Akt2, attenuates the development of pulmonary hypertension. Am J Physiol Lung Cell Mol Physiol. 2015;308:L208–L220. [PubMed: 25416384]

61. Bertero T, Oldham WM, Cottrill KA et al. Vascular stiffness mechanoactivates YAP/TAZ-dependent glutaminolysis to drive pulmonary hypertension. J Clin Invest. 2016;126:3313–3335. [PubMed: 27548520]
62. Majumder P & Baumeister W. in Biological Chemistry Vol. 401 183 (2019). [PubMed: 31665105]
63. Liu S & Martin JF. The regulation and function of the Hippo pathway in heart regeneration. Wiley Interdiscipl Rev Dev Biol. 2019;8:e335.
64. Qin F, Tian J, Zhou D & Chen L. Mst1 and Mst2 kinases: regulations and diseases. Cell Biosci. 2013;3:31–31. [PubMed: 23985272]
65. Foley EA & Kapoor TM. Microtubule attachment and spindle assembly checkpoint signalling at the kinetochore. Nat Rev Mol Cell Biol. 2013;14:25–37. [PubMed: 23258294]
66. Agarwal S & Varma D. How the SAC gets the axe: Integrating kinetochore microtubule attachments with spindle assembly checkpoint signaling. Bioarchitecture. 2015;5:1–12. [PubMed: 26430805]
67. Wang Z, Wan L, Zhong J, Inuzuka H, Liu P, Sarkar FH & Wei W. Cdc20: a potential novel therapeutic target for cancer treatment. Curr Pharm Des. 2013;19:3210–3214. [PubMed: 23151139]
68. Silva PMA, Delgado ML, Ribeiro N et al. Spindly and Bub3 expression in oral cancer: Prognostic and therapeutic implications. Oral Dis. 2019;25:1291–1301. [PubMed: 30866167]
69. Subramanian C & Cohen MS. Over expression of DNA damage and cell cycle dependent proteins are associated with poor survival in patients with adrenocortical carcinoma. Surgery. 2019;165:202–210. [PubMed: 30413320]
70. Al-Tamari HM, Dabral S, Schmall A et al. FoxO3 an important player in fibrogenesis and therapeutic target for idiopathic pulmonary fibrosis. EMBO Mol Med. 2018;10:276–293. [PubMed: 29217661]
71. Kim J, Ishihara N & Lee TR. A DAF-16/FoxO3a-dependent longevity signal is initiated by antioxidants. BioFactors. 2014;40:247–257. [PubMed: 24123695]
72. Chen M, Zhang H, Shi Z et al. The MST4-MOB4 complex disrupts the MST1-MOB1 complex in the Hippo-YAP pathway and plays a pro-oncogenic role in pancreatic cancer. J Biol Chem. 2018;293:14455–14469. [PubMed: 30072378]
73. Dabral S, Muecke C, Valasarajan C et al. A RASSF1A-HIF1α loop drives Warburg effect in cancer and pulmonary hypertension. Nat Commun. 2019;10:2130–2130. [PubMed: 31086178]

Novelty and Significance

What is known?

- Pulmonary arterial hypertension (PAH) is a progressive disease with poor prognosis and no cure.
- Increased proliferation and resistance to apoptosis of resident pulmonary vascular cells lead to the remodeling of small pulmonary arteries and PAH.
- Mammalian STE20-like protein kinases (MST)1/2 are key members of the HIPPO signaling cassette, which act as growth suppressors during development and in adult proliferative diseases.

What new information does this article contribute?

- In contrast to their growth suppressor roles in control cells, MST1 and 2 act as pro-proliferative and pro-survival proteins in PA vascular smooth muscle cells (PAVSMC) and adventitial fibroblasts (PAAF) from patients with PAH.
- In PAH cells, MST1 and 2 form disease-specific interactomes and direct pro-proliferative/pro-survival signaling via BUB3-USP3-dependent activation of Akt and mTOR in PAVSMC and via cytoplasmic retention and degradation of FOXO3 in PAAF.
- Genetic ablation of smooth muscle Mst1/2 reverses pulmonary vascular remodeling and reduces established pulmonary hypertension (PH) in mice.

Hyper-proliferation and resistance to apoptosis of resident pulmonary vascular cells in small PAs are important pathological features of PAH. The serine/threonine proteinkinases MST1/2 are key components of the HIPPO pathway that play growth suppressor roles in health and hyper-proliferative diseases, including human cancers. Our results show that, in contrast to theirgrowth suppressor roles in pulmonary vascular cells from non-diseased lungs, MST1 and 2 function as pro-proliferative/pro-survival modelcules in PAVSMC and PAAF from patients with PAH, and support established pulmonary vascular remodeling and PH in mice. Based on proteomic analysis, we show that MST1/2 have a unique PAH-specific interactome and provide a novel mechanistic link from MST1/2 via BUB3 and FOXO to the abnormal proliferation and survival of PAVSMC and PAAF, PA remodeling and pulmonary hypertension, suggesting potential attractiveness of MST1/2 signaling as a new target pathway for therapeutic intervention in PAH.

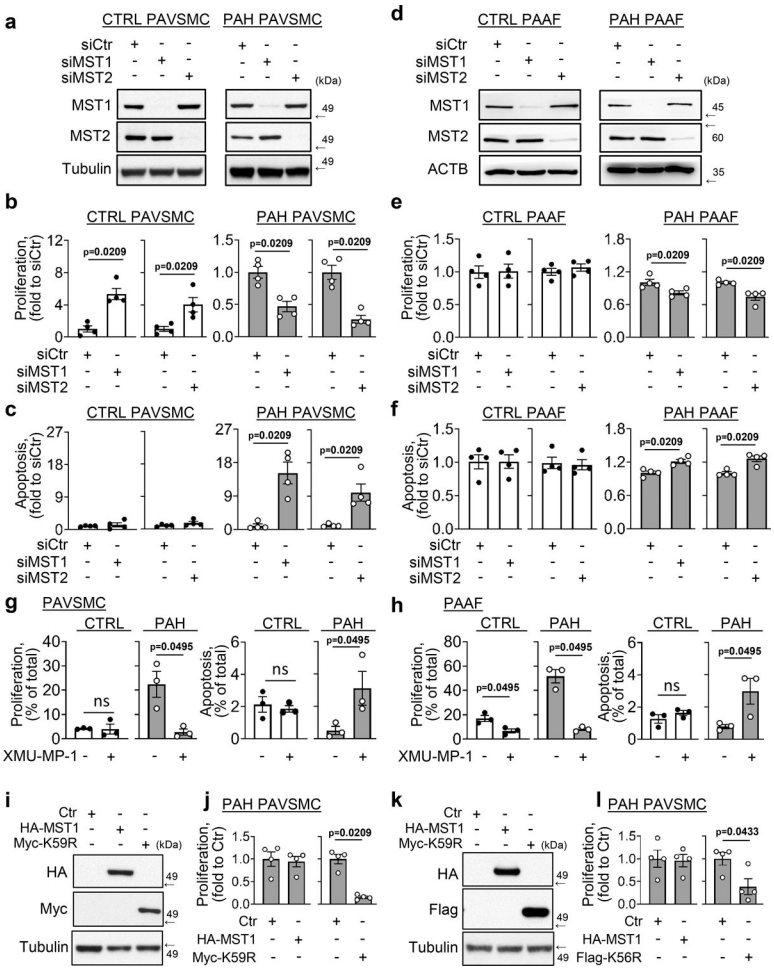

Figure 1. Catalytically active MST1 and MST2 are required for increased proliferation and survival of human PAH PAVSMC and PAAF.

(**a-f**) Early-passage human non-diseased control (CTRL) and PAH PAVSMC (**a-c**) and PAAF (**d-f**) were transfected with small interfering RNA (siRNA) to MST1 or MST2 or scramble siRNA (siCtr) for 48 hours followed by immunoblot analysis (**a,d**), proliferation (BrdU) (**b,e**) and apoptosis (In-situ cell death) analyses (**c,f**). Data represent fold change of BrdU- (**b,e**) or TUNEL-positive cells (**c,f)** relative to siCtr treated cells. See also Supplemental Figure S3 for the statistical analysis of MST1 and MST2 protein levels. (**g,h**) Early-passage human control (CTRL) and PAH PAVSMC (**g**) and PAAF (**h**) were treated with diluent (−) or 5μM XMU-MP-1 (MST1/2 inhibitor) for 48 hours followed by proliferation (Ki67) and apoptosis (TUNEL) analyses. Data represent percentage of Ki67-or TUNEL-positive cells per total number of cells. Data are means±SE from n=4 (b,c,e,f) or n=3 (g,h) subjects per group. **(i-l)** PAH PAVSMC were transfected with control vectors (Ctr) or plasmids expressing human HA-tagged MST1 (HA-MST1), MST2 (HA-MST2), kinase-dead MST1 (Myc-K59R), and kinase-dead MST2 (Flag-K56R) for 48 hours followed by immunoblot analysis (**i, k**) and proliferation (Ki67) (**j, l**) assays. Data are means±SE from n=4 subjects per group. ns-non-significant. P values were calculated by Mann-Whitney U test for independent pairwise comparisons.

PAH-pulmonary arterial hypertension; **PAVSMC**-pulmonary arterial vascular smooth muscle cell; **PAAF**-pulmonary arterial adventitial fibroblast; **TUNEL**-terminal deoxynucleotidyl transferase dUTP nick end labeling; **BrdU**-bromodeoxyuridine.

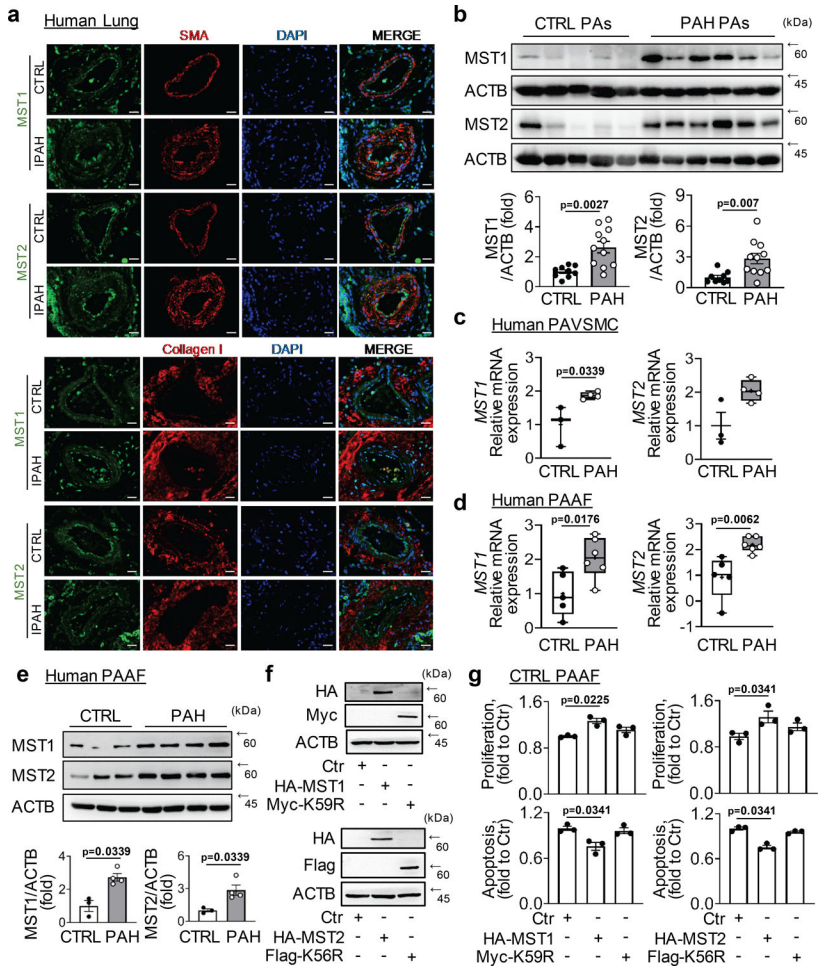

Figure 2. MST1 and MST2 protein levels, mRNA, and distribution in non-diseased and PAH pulmonary vascular cells.

(**a**) Representative immunohistochemical stainings of lung tissue specimens from patients with idiopathic PAH (IPAH) and non-diseased control lungs (CTRL). Green - (MST1 or MST2), red - Collagen I or smooth muscle α-actin (SMA), blue – DAPI. Bar equals 50 μm. Images are representative from n=3 subjects/group. (**b**) Immunoblot analysis of whole pulmonary arteries (PAs) of non-diseased (CTRL) and PAH patients to detect indicated proteins, followed by densitometric analysis. Data are means±SE from n=9 subjects/control, n=11 subjects/PAH group, fold to CTRL; p values were calculated by Mann-Whitney U test. See Supplemental Figure S6A for additional immunoblots used for statistical analysis. (**c-e**). Expression of MST1 and MST2 in human control (CTRL) and PAH PAVSMC (**c**) and PAAF (**d,e**) as analyzed at mRNA level using real time PCRs (**c,d**) and at protein level by immunoblot (**e**). See also supplemental Figure S5. Data are means±SE (**e**) and box and whiskers graph with mean indicated as (+) (**c,d**); (**c**) n=3 subjects/control, n=4 subjects/PAH group; (**d**) n=5 subjects/control, n=6 subjects/PAH group; (**e**) n=3 subjects/control, n=4 subjects/PAH group; p values were calculated by Mann-Whitney U test. (**f, g**) Control (CTRL) PAAF were transfected with control vectors (Ctr) or plasmids expressing human HA-tagged MST1 (HA-MST1), MST2 (HA-MST2), kinase-dead MST1 (Myc-K59R), and kinase-dead MST2 (Flag-K56R) for 48 h followed by immunoblot analysis (**f**) and

proliferation (Ki67) and apoptosis (In-situ cell death) assays (**g**). Data are means±SE from n=3 subjects per group; p values were calculated by Kruskal-Wallis rank test with Dunn's pairwise comparison post-hoc test.

PAH-pulmonary arterial hypertension; **PAVSMC**-pulmonary arterial vascular smooth muscle cell; **PAAF**-pulmonary arterial adventitial fibroblast; **DAPI**-4′,6-diamidino-2-phenylindole.

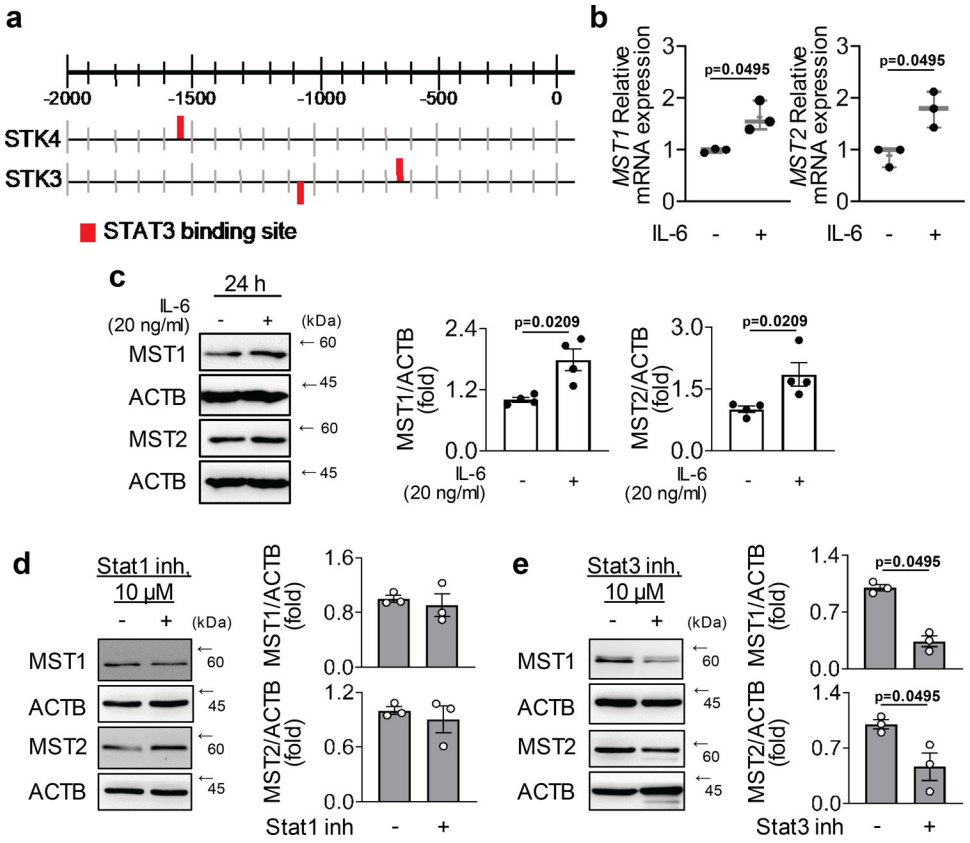

Figure 3. Interleukin-STAT signaling regulates expression of MST1 and MST2 in PAAF.

(**a**) In silico analysis using CiiiDER revealed Stat binding sites in human MST1 (STK4) and MST2 (STK3) promoters. (**b,c**) Non-diseased control PAAF were serum starved for 24 hours followed by IL-6 (20 ng/ml) stimulation for 24 hours and screened for MST1 and MST2 expression at (**b**) mRNA level by real time PCRs and (**c**) protein level by immunoblot analysis. Data are box and whiskers graph with mean indicated as (+) (**b**) and means±SE (**c**) p values were calculated by Mann-Whitney U test. (**d,e**) Human PAH PAAF were treated with vehicle (−) or Stat1/Stat3 inhibitors (10 μM) for 24 hours followed by immunoblot analysis for MST1 and MST2. Data are means±SE; n=3 subjects/group; p values were calculated by Mann Whitney-U test.

PAH-pulmonary arterial hypertension; **PAAF**-pulmonary arterial adventitial fibroblast; **STAT**- Signal transducer and activator of transcription.

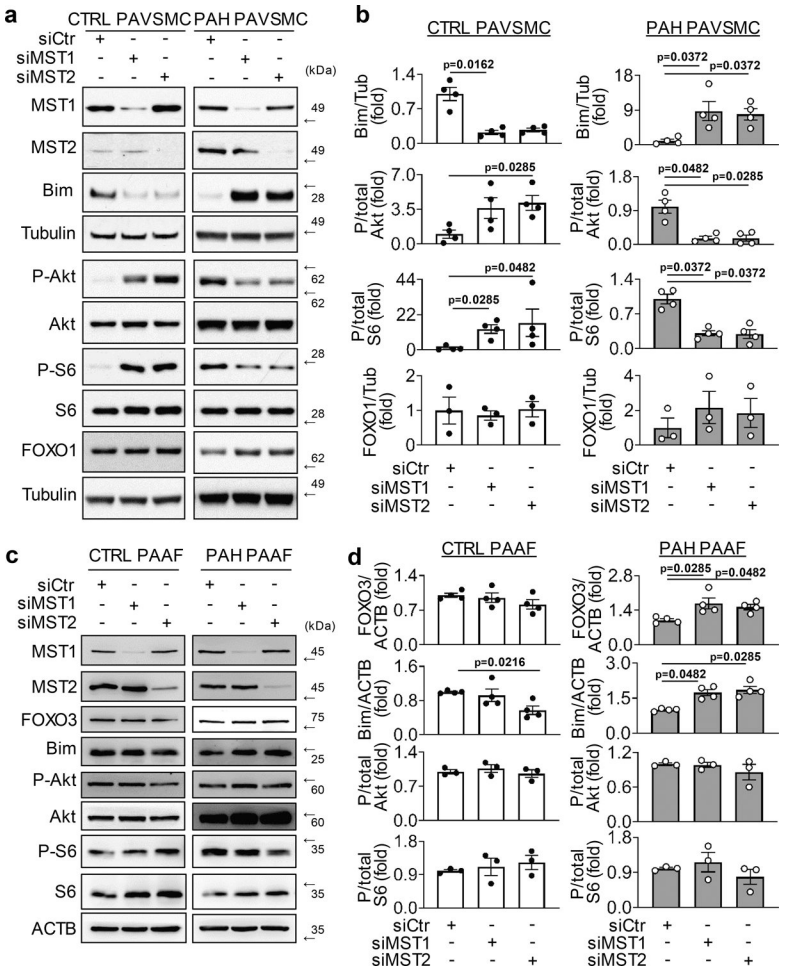

Figure 4. MST1 and MST2 regulates Akt, FOXO and mTOR signaling in human PAH PAVSMC and PAAF.

Early-passage human control (CTRL) and PAH PAVSMC (**a,b**) or PAAF (**c,d**) were transfected with small interfering RNA (siRNA) to MST1 or MST2 or scramble siRNA (siCtr) for 48 hours followed by immunoblot analyses of indicated proteins. (**a,c**) Representative immunoblots are shown. (**b,d**) Data are means±SE; p values were calculated by Kruskal-Wallis rank test with Dunn's pairwise comparison post-hoc test. (**b**) n=4 subjects/group for Bim, P/total Akt, P/total S6; n=3 subjects/group for FOXO1; (**d**) n=4 subjects/group for FOXO3, Bim; n=3 subjects/group for P/total Akt, P/total S6. **PAH**-pulmonary arterial hypertension; **PAVSMC**-pulmonary arterial vascular smooth muscle cell; **PAAF**-pulmonary arterial adventitial fibroblast; **mTOR-** Mammalian target of rapamycin; **FOXO**-forkhead box transcription factors.

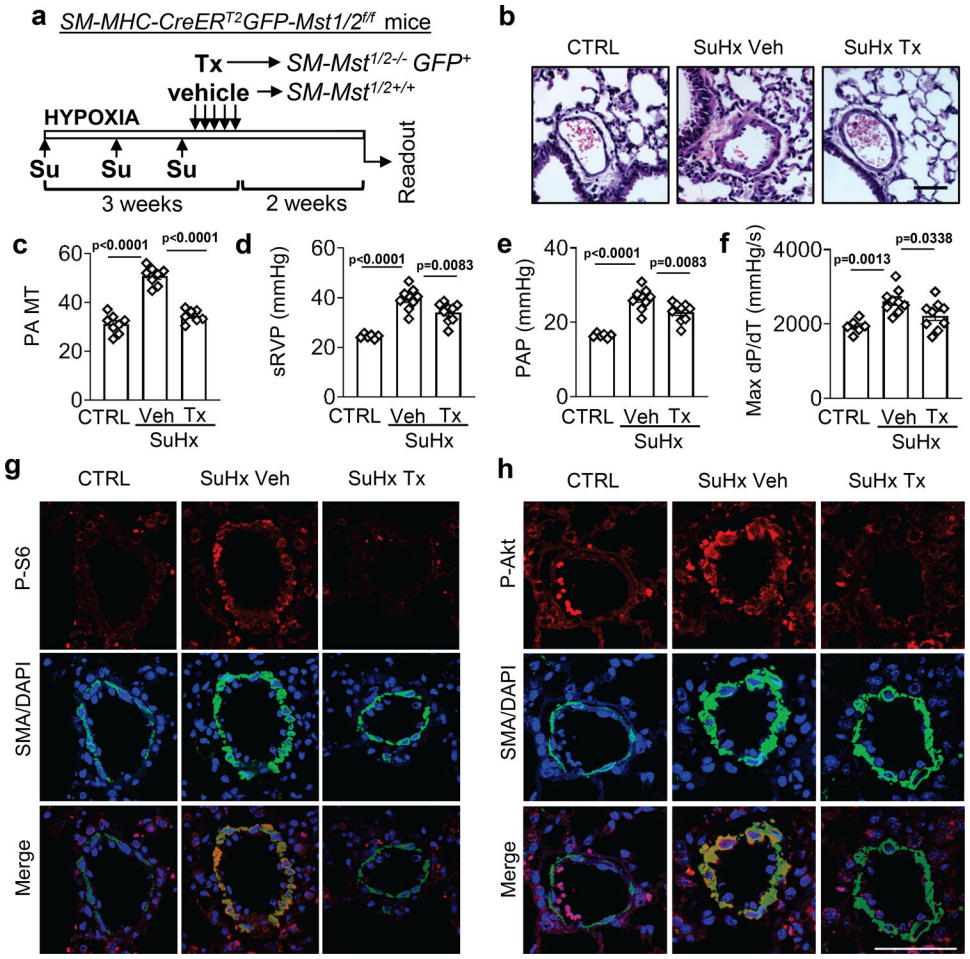

Figure 5. Smooth muscle MST1/2 support established pulmonary vascular remodeling and experimental PH in mice.

(**a**) Schematic representation of the experiment. Mice with SM-specific tamoxifen (Tx)-inducible Mst1/2 knockdown (SM-MHC-CreER^{T2}GFP^{-}Mst1/2$^{fl/fl}$) (see also supplemental Fig. S1 for breeding scheme and characterization) were induced to develop PH by SuHx. At days 17–21 after PH induction, mice received daily Tx to deplete Mst1/2 (SuHx Tx) or vehicle (SuHx Veh) injections and maintained under hypoxia for two more weeks. Controls were normoxia-maintained same-gender littermates (CTRL). (**b,c**) Representative H&E (**b**) and analysis of PA medial thickness (PA MT) (**c**). Bar equals 50 μm. (**d-f**): Statistical analysis of systolic RV pressure (sRVP) (**d**), PA pressure (PAP) (**e**), and RV contractility (max dP/dT) (**f**) analysis of SM-MHC$^{CreERT2/GFP}$Mst1/2$^{fl/fl}$ mice are shown. Data are means±SE, n=8/CTRL, 8/SuHxVeh, 7/SuHxTx mice/group for **c**; 6/CTRL, 9/SuHxVeh, 9/SuHxTx mice/group for **d-f**; p values were calculated by one-way ANOVA with Dunnett's post-hoc test. (**g,h**) IHC stainings of small PAs to detect protein of interest (red)/SMA (green)/DAPI (blue); representative images from 3 mice/group. Bar equals 50 μm. **SM**-smooth muscle; **PH**-pulmonary hypertension; **PA**-pulmonary artery; **RV**- right ventricular; **SuHx** – Sugen Hypoxia.

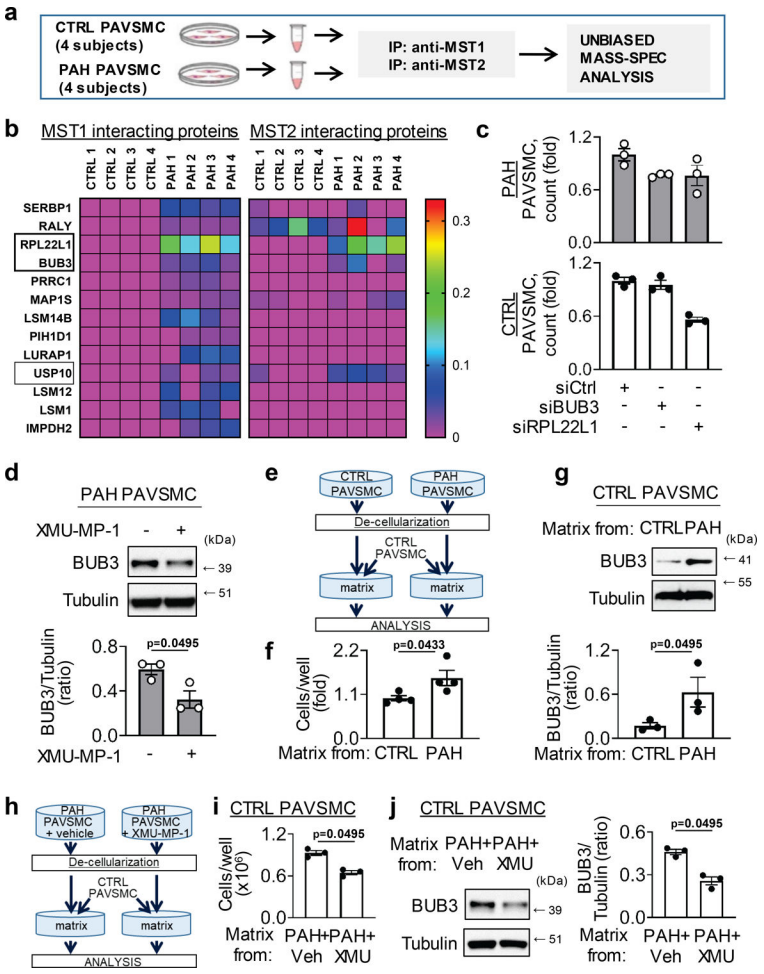

Figure 6. BUB3 is a novel PAH-specific MST1/2-interacting protein in PAH PAVSMC.

(**a**) Schematic representation of mass spec experiment. (**b**) MST1 and MST2 were immunoprecipitated from four non-diseased control (CTRL) and four PAH human PAVSMC followed by mass spec analysis. Left: Heatmap depicting proteins, interacting with MST1 exclusively in PAH but not in non-diseased control (CTRL) PAVSMC. Right: the proteins detected to interact with MST1 exclusively in PAH PAVSMC were also identified among the MST2 interacting proteins. The color intensity scale bar indicates the relative NSAF value of protein-protein interaction. Boxed are proteins showing interaction with both, MST1 and MST2 predominantly in PAH but not CTRL PAVSMC. (**c**) Equal quantity of PAVSMC was plated on 6-well plates; next day, transfection with indicated siRNAs was performed. Cell counts measured 48 hours post-transfection. Data are means±SE, n=3 subjects/group, fold to siCtr. Statistical analysis was performed using Kruskal-Wallis rank test. (**d**) Human PAH PAVSMC were treated with 5 μM XMU-MP-1 or diluent (−) for 48 hours and immunoblot analysis was performed. Data are means±SE from n=3 subjects/group, fold to vehicle (−). (**e-g**) Control (CTRL) or PAH PAVSMC were grown for 7 days. Then cells were removed and equal amount of indicated non-diseased PAVSMC was plated on remaining matrices. 4 days post-plating, (**f**) cell counts and (**g**) immunoblot analysis were performed. Data are means±SE; fold to control cells grown on matrix from CTRL cells;

(**f**) n=4 subjects/group; (**g**) n=3 subjects/group. (**h-j**) PAH PAVSMC were incubated with XMU-MP-1 (XMU) or vehicle for 7 days. Then cells were removed and equal amount of indicated non-diseased cells was plated on remaining matrices. 3 days post-plating, (**i**) cell counts and (**j**) immunoblot analysis were performed. Data are means±SE from n=3 subjects/group, number of cells per well (**i**) and BUB3/Tubulin ratio (**j**) are shown. All p values were calculated by Mann-Whitney U test.

PAH-pulmonary arterial hypertension; **PAVSMC**-pulmonary arterial vascular smooth muscle cell; **NSAF**- normalized spectral abundance factor.

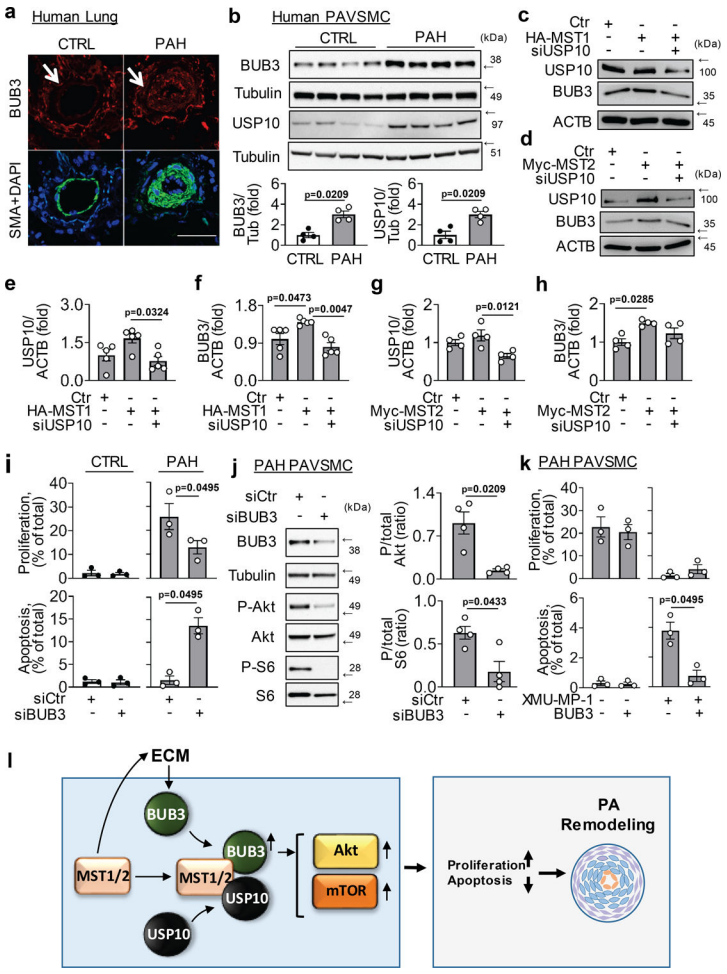

Figure 7. BUB3 selectively supports PAH PAVSMC growth and protects from apoptosis.

(**a**) IHC analysis of non-diseased control (CTRL) and PAH human lungs to detect indicated proteins. Images are representative from 3 subjects/group. Red - BUB3; green - SMA; blue – DAPI. Bar equals 50 μm. (**b**) Immunoblot analysis of PAVSMC from 4 control (CTRL) and 4 PAH human lungs. Data are means±SE, fold to control, p values were calculated by Mann-Whitney U test. (**c-h**) PAH PASMCs were transfected with control vector (Ctr) or plasmids expressing (**c, e, f**) human HA-tagged MST1 (HA-MST1) or (**d, g, h**) MST2 (Myc-MST2) in presence/absence of USP10 siRNA. 48 hours later immunoblot analysis was performed. Data are means±SE from n=5 (**e,f**) or n=4 (**g,h**) subjects per group; p values were calculated by Kruskal-Wallis rank test with Dunn's pairwise comparison post-hoc test. **(i, j)** PAVSMC were transfected with siBUB3, or control scramble (siCtr) siRNA for 48 hours followed by (**i**) proliferation (Ki67), apoptosis (TUNEL) and (**j**) immunoblot analyses. Data are means±SE, percentage of Ki67- or TUNEL-positive cells per total number of cells (**i**) and P/total ratio of indicated proteins, fold to siCtr (**j**) from n=3 (**i**) and n=4 (**j**) subjects/ group, respectively. p values were calculated by Mann-Whitney U test for independent pairwise comparisons. (**k**) PAH PAVSMC were transfected with pCMV6-BUB3 or control pCMV6 plasmid (−) in the presence of XMU-MP-1 (XMU) or diluent (−) for 48 hours, and proliferation (Ki67) and apoptosis (TUNEL) analyses were performed. n=3 subjects/group.

Data are means±SE, percentage of Ki67- (upper panel) or TUNEL-positive cells (lower panel) to the total number of cells, p values were calculated by Mann-Whitney U test for independent pairwise comparisons. (**l**) Schematic representation of proposed function of MST1–2/BUB3 signaling in PAVSMC in PAH.

IHC-immunohistochemistry; **PAH**-pulmonary arterial hypertension; **PAVSMC**-pulmonary arterial vascular smooth muscle cell; **PA**-pulmonary artery; **TUNEL**-terminal deoxynucleotidyl transferase dUTP nick end labeling.

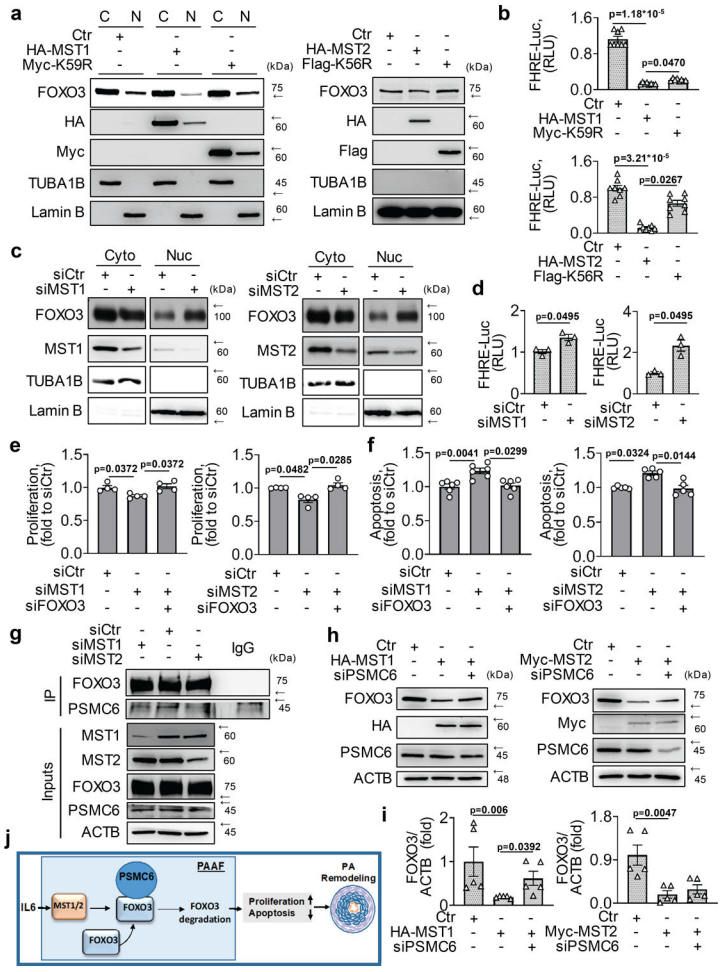

Figure 8. MST1 and MST2 regulate proliferation and survival in PAAF via FOXO3 regulation.

(**a-d**) HEK 293 were transfected with (**a**) control vectors (Ctr) or plasmids expressing HA-MST1, HA-MST2, kinase-dead MST1 (Myc-K59R), and kinase-dead MST2 (Flag-K56R) or (**c**) control siRNA (siCtr), siMST1 and siMST2 for 48 hours followed by subcellular fractionation and immunoblot analysis for indicated proteins. C (Cytoplasm), N (Nucleus). (**b,d**): A luciferase reporter under the control of FoxO response element (FRE) was transfected into the HEK 293 cells with the indicated siRNAs and plasmids as described above for 48 hours followed by measurement of luciferase activity and normalization to renilla luciferase internal control. Data are means±SE; n=8 (**b**) or n=3 (**d**) subjects/group; p values were calculated by Kruskal-Wallis rank test with Dunn's pairwise comparison post-hoc test (**b**) and Mann-Whitney U test for independent pairwise comparisons (**d**). (**e, f**) siCtr, siMST1 and siMST2 were transfected into PAH PAAF with/without FOXO3 siRNA for 48 hours, followed by measurement of (**e**) proliferation (BrdU) and (**f**) apoptosis (In-situ cell death ELISA). Data are means±SE; fold to siCtr, (**e**) n=4 subjects/group; (**f**) n=6 subjects/group (left panel); n=5 subjects/group (right panel); p values were calculated by Kruskal-Wallis rank test with Dunn's pairwise comparison post-hoc test. (**g**) HEK 293 cells were transfected with control siRNA (siCtr), siMST1 and siMST2 with FOXO3-FLAG plasmid for 48 hours. FLAG was immunoprecipitated and co-immunoprecipitated PSMC6

was detected by immunoblot. **(h, i)** HEK 293 were transfected control vectors (Ctr) or plasmids expressing HA-MST1 or Myc-MST2, with or without siPSMC6 for 48 hours followed by immunoblot analysis for indicated proteins, followed by statistical analysis. Data are means±SE; fold to Ctr, n=5 subjects/group, p values were calculated by Kruskal-Wallis rank test with Dunn's pairwise comparison post-hoc test. **(j)** Schematic representation of proposed function of MST1–2/FOXO3 signaling in PAAF in PAH.

PAH-pulmonary arterial hypertension; **PAAF**-pulmonary arterial adventitial fibroblast; **BrdU**-bromodeoxyuridine. **FOXO**-forkhead box transcription factors; **PA**-pulmonary artery.